Combined in situ and remote sensing of ionospheric ion outflow

S. A. Fuselier[1], E. S. Claflin[1], S. B. Mende[2], C. W. Carlson[2], and T. E. Moore[3]

[1]Lockheed Martin Advanced Technology Center, Palo Alto, CA
[2]Space Science Laboratory, University of California, Berkeley, CA
[3]Goddard Space Flight Center, Greenbelt, MD

Abstract: Images of charge-exchanged neutrals from ion outflow during a period of substorm recovery are supported by simultaneous in situ ion outflow measurements and images of the auroral oval. From these combined remote sensing and in situ measurements, the ion outflow is shown to consist of ion conics. The energy of these conics likely increases as they rise out of the Earth's ionosphere. Above ~1.6 R_E, the conic thermal energy is >10 eV while at ~0.7 R_E, it is below this value. The outflow occurs over the entire dayside auroral oval at high latitudes, including the cusp, where auroral emissions are relatively weak. Outflow on the nightside may be weaker than on the dayside and/or may have a different energy-altitude dependence.

Introduction

Polar orbiting spacecraft have observed ionospheric ion outflow (e.g., H^+, He^+, and O^+) along high latitude field lines for decades (see, e.g., Yau et al., [1985]). These snapshots in space and time have been assembled in a statistical fashion to determine many properties of the outflow. For example, statistical studies show that the outflow flux is proportional to magnetospheric activity and solar cycle [Yau et al., 1985]. More recent statistical studies of outflow indicate that the fluxes scale directly with the pointing flux into the ionosphere and with the "soft" electron density (i.e., the density of precipitating electrons with energies below about 1 keV) [Strangeway et al., 2005].

Two types of ion outflow distributions with distinct pitch angle characteristics and energies of 10s of eV are typically observed. The first type, ion beams, has peak flux along the magnetic field and the second type, ion conics, has peak flux at an angle to the magnetic field. Ion conics have been the focus of intense study because their properties provide clues to the acceleration mechanisms that extract them from the ionosphere.

There are two types of ion conics: restricted and extended. Extended (or bi-modal) conics have significant bulk velocity (10s of km/s) along the magnetic field as well as significant perpendicular thermal velocity (also 10s of km/s). Restricted conics have similar perpendicular thermal velocity, but low bulk velocity along the magnetic field. Statistical studies show that restricted conics occur in the auroral zone between invariant latitude 65-85°, at all local times, but peaked on the morning/dayside between 5 and 13 magnetic local time (MLT), and at altitudes from ~1R_E to >4R_E [Miyake et al., 1996]. Over this range of altitudes, conic angles (the peak flux angle relative to the magnetic field) are nearly constant [Peterson et al., 1992]. Since the magnetic field strength decreases dramatically from 1 to 4 R_E altitude, there must be continuous perpendicular energization to maintain the constant pitch angle with altitude. Extended conics are less common than restricted conics, have similar latitude dependence and conic angle dependence with altitude, and show a more uniform occurrence frequency with MLT. Finally, outflow studies typically focus on O^+ or He^+; however, the properties of H^+ conics are similar.

In situ measurements have revealed important statistical properties of ion outflow. However, the nature of these in situ snapshots at a single MLT and altitude, taken over a few minutes, precludes determining the temporal and spatial variation of ion outflow over important timescales (such as the substorm timescale of about 1 hour). Statistical studies show that ionospheric ion outflow [Yau et al., 1985] and ionospheric ions in the plasma sheet [e.g., Lennartsson, 1992] are both dependent on magnetospheric activity. Thus, there is a strong indication that the ionosphere influences the plasma content of the plasma sheet (and ring current) over the course of a substorm.

This lack of resolved spatial and temporal information over the substorm timescale has led to two disparate models for the outflow that ultimately populates the plasma sheet. The first model has the plasma sheet supplied by outflow from the entire auroral oval, with approximately equal contributions from the dayside and nightside [Shelley et al., 1985]. The second model has the plasma sheet supplied largely by outflow from the dayside cusp region [Moore et al., 1985]. Neither model predicts when the outflow will occur, only that it must increase early in the substorm process. Recent statistical studies have not been able to distinguish between these models. They show that there is significant Poynting flux (and ion outflow) into both the dayside and nightside auroral zone [Zheng et al., 2005], and, in particular, into the cusp region [Lennartsson et al., 2004].

As the outflow propagates along the magnetic field line, a fraction of the ions charge exchange with the geocorona. If the resulting neutral atoms have energies >10 eV, then they can be imaged with the low energy neutral atom (LENA) imager on the IMAGE spacecraft [Moore et al., 2000]. Ideally, the images can be inverted to determine the global properties of the parent ion population. In practice, this inversion process has proven difficult because of the inherent characteristics of the parent outflow distributions [Fuselier et al., 2002]. In particular, it is difficult to determine whether changes in the observed neutral flux are due to changes in intensity, temperature (energy), charge exchange altitude, and/or pitch angle of the parent ion population. Of these, the pitch angle and energy appear to be very important [Fuselier et al., 2002].

This paper reports a combination of neutral atom imaging, in situ measurements of ion outflow, and auroral imaging that eliminates much (but not all) of the uncertainty associated with using only one of these techniques.

Ion Outflow Observations

Figure 1 shows the auroral intensity observed by the IMAGE/FUV Wideband Imaging Camera (WIC) [Mende et al., 2000] on 27 November 2000 at 0212 UT. When this image was taken, the spacecraft was located on the dawnside at about 4 R_E altitude. The auroral oval is shown in MLT – invariant latitude coordinates with noon at the top and dusk to the left. A large section of the oval from about 18 to 23 MLT is missing because, at this relatively low altitude, the WIC field-of-view does not cover the entire oval. The WIC detects emissions between 140 and 180 nm, produced mainly by precipitating electrons. In addition, dayglow emissions are seen from 9 to 15 MLT up to the terminator (at about 60° invariant latitude). The auroral oval is extensive, stretching from 60° to ~80° invariant latitude over almost all local times except at noon. This extended oval is typically observed during the substorm recovery phase [e.g., Mende et al., 2004].

During these auroral observations, the Fast Auroral SnapshoT (FAST) spacecraft traversed the dawnside oval at an altitude of ~4000 km (see the arrow in Figure 1). Figure 2 shows in situ observations of ion and electron precipitation and ion outflow from the FAST spacecraft along this trajectory. The four panels show (top to bottom) the precipitating ion flux (in an energy-time format), the precipitating electron flux, the ionospheric ion outflow, and the pitch angle versus time of the ionospheric outflow. From 0204 to 0213 UT, the FAST spacecraft traversed the auroral oval from low latitude to high latitude. In the oval, there is ion precipitation at energies above 100 eV. The poleward edge of the oval has intense fluxes of soft (energies <1000 eV) electron precipitation and ionospheric ion outflow at energies primarily <10 eV. The dot along the FAST spacecraft trajectory in Figure 1 shows where this intense outflow was observed. (The apparent intense fluxes in Figure 2 at 0220 UT in the polar cap are a spacecraft charging effect and are not outflow.) The pitch angle plot in Figure 2 shows that the intense ion outflow at 0212 UT is characterized by high fluxes at ~132° from the magnetic field (i.e., the ion outflow distributions are conics). Ion conics at the poleward edge of the oval are observed during substorm recovery [e.g., Mende et al., 2004] and are associated with soft electron precipitation [Strangeway et al., 2005].

The left hand panel of Figure 3 shows a neutral atom image from the LENA imager for the period from 0156 to 0210 UT (near the FAST spacecraft traversal of the auroral oval). Plotted are the counts/s of neutral atoms from ~10 eV to >300 eV. The view perspective is from the IMAGE spacecraft location on the dawnside. Magnetospheric magnetic field lines at L-shells of 2 and 4 are shown in the sunward direction (lower right hand corner), duskward (upper right), tailward (upper left), and dawnward (lower left). Neutralized ionospheric ions (i.e., ions that charge exchange with the geocorona) are seen at all MLTs, but the most intense neutral fluxes encircle approximately half the Earth from 6 to 18 MLT. This type of neutral flux is often seen when the IMAGE spacecraft is post-perigee during a substorm recovery interval.

Some of the neutral atoms seen by the IMAGE spacecraft are associated with the ionospheric ion outflow observed by the FAST spacecraft. The FAST spacecraft traversed the auroral oval at about 9 MLT (Figure 1). It observed intense conic outflow at energies <10 eV at the edge of the auroral oval. This ion outflow propagates along magnetic field lines projected out from the ionosphere at 9 MLT (see Figure 4). Outflow from this region that is energized to >10 eV and that charge exchanges at high altitudes (~2-3 R_E) would appear in the lower middle part of the LENA image in Figure 3, between the sunward and dawnward magnetic field lines. Figure 4 shows that the apparent direction of arrival of these charge-exchanged neutrals would be offset from the Earth direction. Thus, there is a direct association between the intense outflow seen at low altitudes by the FAST spacecraft and the charge exchanged neutrals from high altitudes in the lower middle part of the LENA image.

Simple Model of Ionospheric Outflow

The LENA image in Figure 3 also shows charge-exchanged ionospheric outflow comes from other parts of the auroral oval. To determine the origin of these neutrals, a simple ion outflow model is used to obtain the synthetic neutral atom image in the right hand panel of Figure 3. To obtain this synthetic image, five assumptions were made. First, it was assumed that ionospheric outflow occurs over all local times at invariant latitude >70° in proportion to the intensity of the auroral oval in FUV/WIC image in Figure 1. The basis for this assumption is that the FAST spacecraft observed intense outflow at latitudes >70° in association with the edge of the oval (Figure 1). Second, it was assumed that the all outflow distributions were ion conics with conic angle = 132±30°. The basis of this assumption was the in situ observations of ion conics with this conic angle (Figure 2). Third, it was assumed that the conic angle remained fixed for all altitudes. The basis for this assumption was the statistical observations of fixed ion conic angles [Peterson et al., 1992]. Fourth, it was assumed that the charge-exchange cross section does not depend on energy from ~10 – 100 eV. Finally, the fifth assumption was that charge exchange for energies >10 eV did not occur below 1.6 R_E altitude. The basis for this assumption was the empirical comparison of the synthetic outflow image in the right hand panel of Figure 3 with the outflow image from LENA in the left hand panel. One possible explanation for this empirical result is that the ion conics must be energized to energies >10 eV between the altitude of the FAST orbit (~0.7 R_E) and ~1.6 R_E.

With these assumptions, the auroral intensity at latitudes >70° was used as a proxy for the ion outflow intensity and this outflow was assumed to charge exchange as it propagated along the model magnetic field lines. The altitude dependence of the geocoronal density (from the model by Østgaard et al. [2003], modified to be valid below 3.5 R_E) was used to determine what portion of the outflow intensity was charge exchanged at each altitude (above 1.6 R_E). The resulting neutrals are not confined by the magnetic field lines and propagate in straight lines, forming a series of cones centered on the magnetic field at 132±30° (i.e., the conic angle). Figure 4 shows a 2-dimensional projection of this 3-dimensional geometry for the field line associated with the outflow observed by the FAST spacecraft. Adding up the line of sight fluxes from all the neutral “cones” (originating on all field lines) that intersect the LENA imager field of view created the final synthetic image in the right hand panel of Figure 3.

The LENA image and the synthetic image of outflow in Figure 3 have similarities and some significant differences. Both images show neutral atom flux that peaks in a line of sight direction that is offset from the Earth direction. This similarity is a consequence of the choice of the 1.6 R_E minimum charge exchange altitude. If this altitude were significantly lower, then the line of sight flux in the synthetic image would appear in the Earth direction. Thus, the peak flux offset from the Earth direction must come from ion outflow at energies >10 eV that charge exchanges at high altitudes.

The local time characteristics of the LENA and synthetic images in Figure 3 are significantly different. In the LENA image, outflow is concentrated on the dayside. The synthetic image reflects the more complicated local time characteristics of the auroral oval at latitudes >70°. In particular, the noontime gap in the synthetic image is indicative of the lack of auroral emissions near noon. The significant line of sight neutral atom flux in the LENA image indicates that there is also significant ion conic outflow from the cusp region that charge exchanges at high altitudes. This flux must rival the fluxes seen by the FAST spacecraft at about 9 MLT.

The greatest difference between the LENA and synthetic images is seen in the comparison of the dayside and nightside fluxes. In the synthetic image, the flux peaks on the nightside near midnight while the LENA image shows the peak flux on the dayside over a broad range from 6 to 18 MLT. The lower nightside fluxes indicate that there is a substantial difference in the ionospheric outflow from the poleward edge of the nightside auroral oval when compared to the dayside, despite the more intense auroral emissions on the nightside.

Although only a single LENA image is shown in Figure 3, it is representative of images obtained over the time interval from 0100 – 0230 UT on 27 November 2000. The IMAGE spacecraft altitude increased from 3.6 to 5.8 R_E during this interval. Despite the altitude change and the change in view perspective, the apparent arrival direction of the neutral flux continued to be offset from the Earth direction as in the left hand panel of Figure 3.

Discussion

Using in situ observations from the FAST spacecraft (Figure 2) of ion outflow from the poleward edge of the auroral oval as a guide, the arrival direction of the neutrals (Figure 3, left hand panel) is consistent with high altitude charge exchange of ion outflow from the poleward edge of the auroral oval over nearly the entire dayside. The neutral arrival direction indicates that the LENA imager is not seeing charge-exchange outflow below ~1.6 R_E altitude. Charge exchange is certainly taking place at lower altitudes, where the geocorona is denser. However, if the parent ion population has energies <10 eV, then the resulting neutrals will be below the ~10 eV low energy cutoff of the LENA imager. Indeed, the intense outflow seen by the FAST spacecraft at ~0.7 R_E has peak energies < 10 eV. These observations suggest that ion conics are energized from energies <10 eV at ~0.7 R_E to >10 eV at ~1.6 R_E.

The comparison between the LENA image and synthetic image in Figure 3 shows that the properties of ion outflow are not strongly correlated with the auroral oval intensity. In particular, the nightside aurora is intense but the neutral flux is weak and the cusp aurora is weak but the neutral flux is intense. The lack of correlation is rooted in the difficulty in distinguishing aurora created by high-energy electron precipitation (with correspondingly weak outflow) and low-energy electron precipitation (with correspondingly intense outflow) (see Mende et al. [2004]).

For the nightside, it may be that the weaker neutral flux may be the result of weaker ion outflow during this substorm recovery interval. Unfortunately, this explanation is not unique. The weaker nightside neutral flux could be the result of a different energy-altitude dependence and/or a different pitch angle dependence to the ion outflow. If nightside ion outflow was as intense as the dayside, but the ions never attained energies >10 eV, then the bulk of the neutral flux would be below the low energy cutoff of the LENA imager. If the outflow distributions were field-aligned beams, then the resulting charge-exchanged population would not be directed into the LENA field of view. Thus, without simultaneous in situ measurements in the nightside region, the differences between dayside and nightside ion outflow cannot be resolved for this event.

Although the local time and latitudinal intensity of the auroral oval emissions are not good indicators of ion outflow, the total auroral intensity (summed over the entire oval) remains a good indicator of ion outflow. Neutral atom images from the IMAGE orbits before and after the substorm recovery interval in Figure 3 (not shown here) indicate much weaker neutral fluxes.

During these intervals, the geomagnetic activity was low and the auroral emissions were also weak.

The observations show that, at least for substorm recovery, the entire dayside auroral region and not just the cusp region produces these ionospheric ions. These data do not necessarily distinguish the relative contributions of the dayside and nightside except to indicate that, at energies >10 eV, the dayside flux of charge-exchanged ion conics is higher than the nightside flux. Further work is needed to correlate neutral atom images and ion outflow with other phases of the substorm cycle.

Acknowledgements: The IMAGE mission is the result of the work of a large number of dedicated scientists and engineers. J. Burch is the PI for the IMAGE mission. Research at Lockheed Martin was supported by contract from Goddard Space Flight Center and by subcontract from the University of California, Berkeley.

References:

Fuselier, S. A., et al., Localized ion outflow in response to a solar wind pressure pulse, *J. Geophys. Res., 107*, doi: 10.1029/2001JA000297, 2002.

Lennartsson, O. W., A scenario for solar wind penetration of Earth's magnetic tail based on ion composition data from the ISEE 1 spacecraft, J. Geophys. Res., 97, 19,222, 1992.

Lennartsson, O. W., H. L. Collin, and W. K. Peterson, Solar wind control of Earth's H^+ and O^+ outflow rates in the 15-eV to 33-keV energy range, *J. Geophys. Res.,* A122212, 2004.

Mende, S. B., et al., Far ultraviolet imaging from the IMAGE spacecraft. 2. Wideband FUV imaging, in *The IMAGE Mission*, ed. J. L. Burch, Kluwer Academic Publishers, Dordrecht, p. 271-285, 2000, *Space Sci. Rev., 91*, 271-285, 2000.

Mende, S. B., et al., IMAGE FUV and in situ FAST particle observations of substorm aurorae, *J. Geophys. Res., 108(A4),* 8010, doi: 10.1029/2002JA009413, 2003.

Miyake, W., T. Mukai, and N. Kaya, On the origins of the upward shift of elevated (bimodal) ion conics in velocity space, *J. Geophys. Res., 101*, 26,961, 1996.

Moore, T. E., C. R. Chappell, M. Lockwood, and J. H. Waite, Jr., Superthermal ion signatures of auroral acceleration processes, *J. Geophys. Res., 90,* 1611, 1985.

Moore, T. E., et al., The low-energy neutral atom imager for IMAGE, in *The IMAGE Mission*, ed. J. L. Burch, Kluwer Academic Publishers, Dordrecht, p. 155-195, 2000.

Østgaard, et al., Neutral hydrogen density profiles derived from geocoronal imaging, *J. Geophys. Res., 108,* 1300, 2003.

Peterson, W. K., H. L. Collin, M. F. Doherty, and C. M. Bjorklund, O^+ and He^+ restricted and extended (bi-modal) ion conic distributions, *Geophys. Res. Lett., 19,* 1439, 1992.

Shelley, E. G., Circulation of energetic ions of terrestrial origin in the magnetosphere, *Adv. Space Res., 5,* 401, 1985.

Strangeway, R. J., et al., Factors controlling ionospheric outflows as observed at intermediate altitudes, *J. Geophys. Res.,* in press, 2005.

Yau, A. W., P. H. Beckwith, W. K. Peterson, and E. G. Shelley, Long-term (solar cycle) and seasonal variations of upflowing ionospheric ion events at DE 1 altitudes, *J. Geophys. Res., 90,* 6395, 1985.

Zheng, Y., et al., Polar study of ionospheric ion outflow versus energy input, *J. Geophys. Res.,* submitted, 2005.

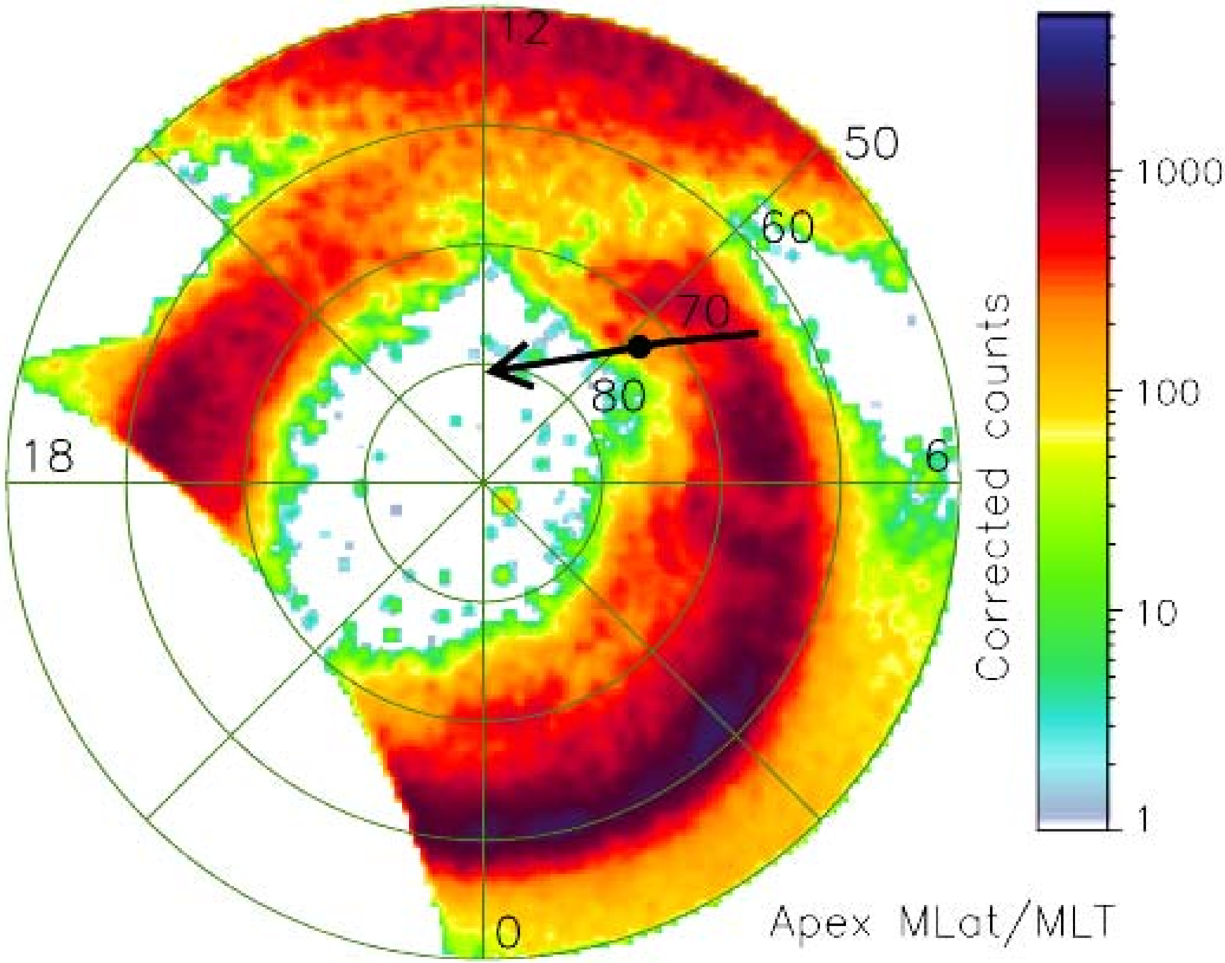

Figure 1. Auroral oval on 27 November 2000. The oval is broad during this substorm recovery interval. The black arrow is the footprint of the FAST spacecraft trajectory. At the dot on this trajectory, intense ion outflow was observed.

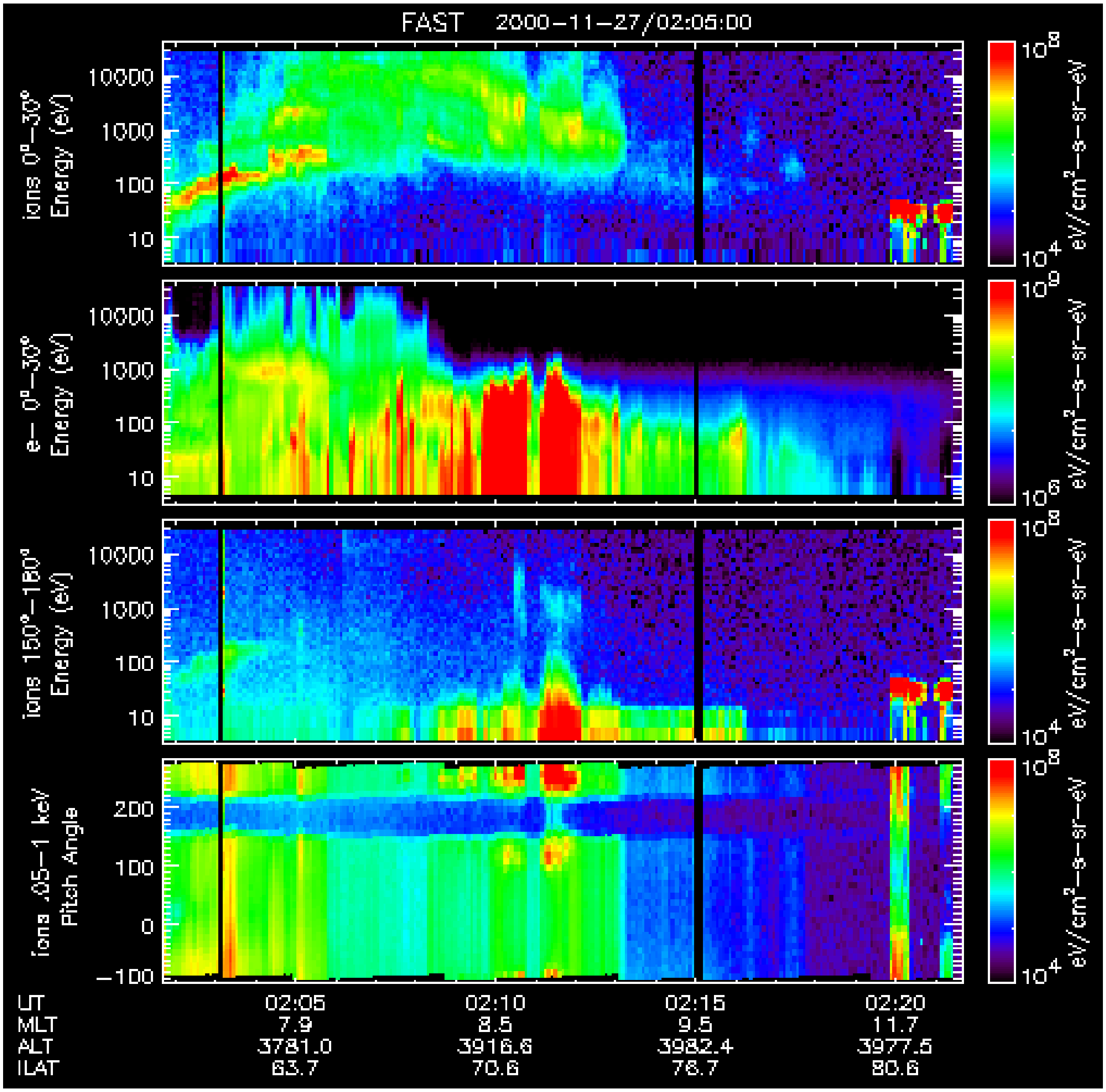

Figure 2. FAST spacecraft in situ observations. (Top to bottom) ion precipitation, electron precipitation, ion outflow from the ionosphere, and pitch angles of the ion outflow. In the auroral oval (from 0202 and 0213 UT) there is intense, high-energy ion precipitation and intense high and low energy electron precipitation. Intense low energy electron precipitation occurs near the poleward edge of the oval and is associated with peak ion outflow (ion conics) at energies <10 eV.

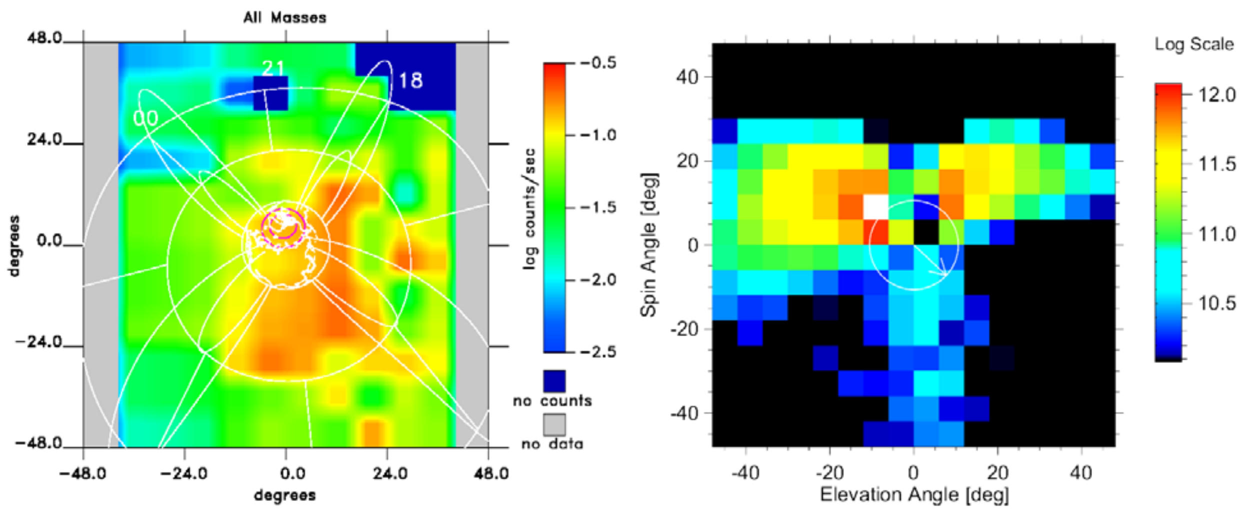

Figure 3. (Left) Neutral atom image viewed from the LENA imager perspective. Noon (dusk) is in the lower right (left) hand corner. The neutral flux peaks over the entire dayside off the direction to the Earth. (Right) synthetic neutral atom image (see text).

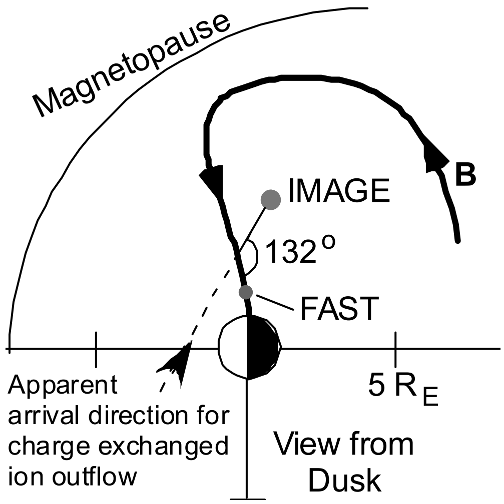

Figure 4. Duskside view of the magnetic field line associated with intense ion outflow. The outflow conics make an angle of 132° with the magnetic field. Charge exchange at altitudes above the FAST spacecraft results in an apparent arrival direction at IMAGE that is offset from the Earth direction.